Dipolar Bose-Einstein condensates at finite temperature

Shai Ronen
JILA and Department of Physics, University of Colorado, Boulder, Colorado 80309-0440, USA

John L. Bohn*
JILA, NIST, and Department of Physics, University of Colorado, Boulder, Colorado 80309-0440, USA

(Received 4 July 2007; published 8 October 2007)

We study a Bose-Einstein condensate of a dilute gas with dipolar interactions, at finite temperature, using the Hartree-Fock-Bogoliubov theory within the Popov approximation. An additional approximation involving the dipolar exchange interaction is made to facilitate the computation. We calculate the temperature dependence of the condensate fraction of a condensate confined in a cylindrically symmetric harmonic trap. We show that the biconcave-shaped condensates found in [Ronen *et al.* Phys. Rev. Lett. **98**, 30406 (2007)] in certain pancake traps at zero temperature are also stable at finite temperature. Surprisingly, the dip in the central density of these structured condensates is actually enhanced at low finite temperatures. We explain this effect.

DOI: 10.1103/PhysRevA.76.043607 PACS number(s): 03.75.Hh

I. INTRODUCTION

The realization of a Bose-Einstein condensate (BEC) of ^{52}Cr [1] marked a major development in degenerate quantum gases in that the interparticle interaction via magnetic dipoles in this BEC is much larger than that in alkali-metal atoms and leads to an observable change in the shape of the condensate. The long-range nature and anisotropy of the dipolar interaction pose challenging questions about the stability of the BEC and have led to predictions of unique phenomena, such as roton-maxon spectra, different phases of vortex lattices, biconcave-shaped condensates, and novel spin textures [2–16].

The effect of finite temperature on these phenomena, or new temperature-dependent effects, remains largely unexplored. Theoretical finite-temperature studies have been confined to path-integral Monte Carlo simulations [9] of a small number (100) of particles and to a homogeneous, quasi-one-dimensional (quasi-1D) system [17]. In the latter work, the Popov approximation to the Hartree-Fock-Bogoliubov (HFB) theory has been applied [18,19]. In systems with short-range interactions, the Popov approximation has been found to give excitation spectra in good agreement with experiment for temperatures up to half the critical temperature for condensation [20]. For the density profile, good accuracy was shown for even higher temperatures, up to the critical temperature.

In [13] we have introduced a computational algorithm which allowed us to calculate the Bogoliubov excitation spectrum of dipolar condensates in cylindrically symmetric 3D traps at zero temperature. Here we extend this work in a natural way to describe finite-temperature properties in the Popov approximation. In essence, the Popov approximation is a self-consistent solution in which the Bogoliubov excitation spectrum is computed and the different excitation modes populated according to Bose statistics. This leads to depletion of the condensate and thus a shift in excitation frequencies. The excitation spectrum is recalculated iteratively until self-consistency is achieved.

II. FORMALISM

The HFB-Popov equations for the case of short-range interactions have been described by Griffin [18]. The generalization to long-range interactions is straightforward, and we therefore briefly formulate it in this section. The confined Bose gas is portrayed as a thermodynamic equilibrium system under the grand-canonical ensemble whose thermodynamic variables are the temperature T and the chemical potential μ. There is a one-to-one relationship between the chemical potential μ and the total number of particles, N. Below the critical temperature, N_0 of the atoms are in a condensate state. The system Hamiltonian K for the system with a fixed chemical potential is then obtained from the Hamiltonian H of the system with fixed number of total particles via a Legendre transform and has the form

$$K = H - \mu N = \int d\boldsymbol{r}\hat{\Psi}^\dagger(\boldsymbol{r})(H_0 - \mu)\hat{\Psi}(\boldsymbol{r}) + \frac{1}{2}\int \hat{\Psi}^\dagger(\boldsymbol{r})\hat{\Psi}^\dagger(\boldsymbol{r}')V(\boldsymbol{r}' - \boldsymbol{r})\hat{\Psi}(\boldsymbol{r}')\hat{\Psi}(\boldsymbol{r}), \quad (1)$$

where $\hat{\Psi}(\boldsymbol{r})$ is the Bose field operator that annihilates an atom at position $\boldsymbol{r}$, $H_0=(-\hbar^2/2M)\nabla^2+V_{trap}(\boldsymbol{r})$ contains the kinetic energy and the trap potential, and $V(\boldsymbol{r})$ is the particle-particle interaction potential. For the system treated here, the trap potential is cylindrically symmetric: $V_{trap}(\boldsymbol{r})=M(\omega_\rho^2\rho^2+\omega_z^2z^2)/2$, where M is the atomic mass and ω_ρ and ω_z are the radial and axial trap frequencies, respectively. For polar gases the potential $V(\boldsymbol{r})$ may be written

$$V(\boldsymbol{r}) = \frac{4\pi\hbar^2 a}{M}\delta(\boldsymbol{r}) + d^2\frac{1-3\cos^2\theta}{r^3}, \quad (2)$$

where a is the scattering length, d the dipole moment, $\boldsymbol{r}$ the distance between the dipoles, and θ the angle between the

*bohn@murphy.colorado.edu

vector $\boldsymbol{r}$ and the direction of polarization, which is aligned along the trap z axis.

The Bose field operator is decomposed into a c-number condensate wave function plus an operator describing the noncondensate part, $\hat{\Psi}(\boldsymbol{r})=\sqrt{N_0}\phi(\boldsymbol{r})+\tilde{\psi}(\boldsymbol{r})$, and inserted into Eq. (1). Terms cubic and quartic in $\tilde{\psi}(\boldsymbol{r})$ are treated within the mean-field approximation and the grand-canonical Hamiltonian reduces to a sum of three terms: $K=K_0+K_1+K_2$. The first term K_0 is a c number, the second term K_1 is linear in $\tilde{\psi}(\boldsymbol{r})$ (and its Hermitian conjugate), and the last term K_2 is quadratic in these quantities. Within the Popov approximation, the so-called anomalous terms arising from mean field averages of the form $\langle\tilde{\psi}\tilde{\psi}\rangle$ are ignored and only "normal" terms of the form $\langle\tilde{\psi}^\dagger\tilde{\psi}\rangle$are included [18]. For a system in equilibrium the linear term K_1 is required to vanish identically, giving a generalized Gross-Pitaevskii (GP) equation for $\phi(\boldsymbol{r})$:

$$\left[H_0+\int d\boldsymbol{r}' N_0|\phi(\boldsymbol{r}')|^2+\tilde{n}(\boldsymbol{r}')V(\boldsymbol{r}'-\boldsymbol{r})\right]\phi(\boldsymbol{r})+\int\tilde{n}(\boldsymbol{r}',\boldsymbol{r})V(\boldsymbol{r}'-\boldsymbol{r})\phi(\boldsymbol{r}')=\mu\phi(\boldsymbol{r}),\tag{3}$$

where $\tilde{n}(\boldsymbol{r})\equiv\langle\tilde{\psi}^\dagger(\boldsymbol{r})\tilde{\psi}(\boldsymbol{r})\rangle$ is the density of the noncondensate (thermal) atoms and $\tilde{n}(\boldsymbol{r}',\boldsymbol{r})\equiv\langle\tilde{\psi}^\dagger(\boldsymbol{r}')\tilde{\psi}(\boldsymbol{r})\rangle$ is the one-particle reduced density matrix, or the correlation function, of the noncondensate atoms. The term involving $\tilde{n}(\boldsymbol{r})$ represents the mean-field contribution due to direct interaction between the thermal cloud and the condensate. The term involving $\tilde{n}(\boldsymbol{r}',\boldsymbol{r})$ represents the contribution of exchange interaction between the thermal cloud and the condensate. Note that for V with only short-range interaction, the exchange term reduces in form to that of the direct one. But for long-range interaction, the nonlocal correlation function is needed. Also, note that a more careful treatment [21,22] reveals that, for an atom-number-conserving system, the factor N_0 in Eq. (3) should be replaced by N_0-1. This correction is negligible for $N_0>>1$.

The term K_2 has the form

$$K_2=\int d\boldsymbol{r}\tilde{\psi}^\dagger(\boldsymbol{r})\mathcal{L}\tilde{\psi}(\boldsymbol{r})+\int d\boldsymbol{r}d\boldsymbol{r}'\tilde{\psi}^\dagger(\boldsymbol{r}')n(\boldsymbol{r},\boldsymbol{r}')V(\boldsymbol{r}'-\boldsymbol{r})\tilde{\psi}(\boldsymbol{r})+\frac{N_0}{2}\int d\boldsymbol{r}d\boldsymbol{r}'\tilde{\psi}^\dagger(\boldsymbol{r}')\tilde{\psi}^\dagger(\boldsymbol{r})V(\boldsymbol{r}'-\boldsymbol{r})\phi(\boldsymbol{r})\phi(\boldsymbol{r}')+\frac{N_0}{2}\int d\boldsymbol{r}d\boldsymbol{r}'\tilde{\psi}(\boldsymbol{r}')\tilde{\psi}(\boldsymbol{r})V(\boldsymbol{r}'-\boldsymbol{r})\phi^*(\boldsymbol{r})\phi^*(\boldsymbol{r}'),\tag{4}$$

where $\mathcal{L}=H_0-\mu+\int d\boldsymbol{r}'V(\boldsymbol{r}'-\boldsymbol{r})n(\boldsymbol{r}')$, in which $n(\boldsymbol{r}')=\tilde{n}(\boldsymbol{r}')+N_0|\phi(\boldsymbol{r}')|^2$ is the total density and $n(\boldsymbol{r},\boldsymbol{r}')=\tilde{n}(\boldsymbol{r},\boldsymbol{r}')+N_0\phi^*(\boldsymbol{r})\phi(\boldsymbol{r}')$ is the total correlation function.

The term K_2 can be diagonalized by the Bogoliubov transformation

$$\tilde{\psi}(\boldsymbol{r})=\sum_j[u_j(\boldsymbol{r})\alpha_j+v_j^*(\boldsymbol{r})\alpha_j^\dagger]\tag{5}$$

if the quasiparticle amplitudes $u_j(\boldsymbol{r})$ and $v_j(\boldsymbol{r})$ satisfy the coupled HFB-Popov equations

$$E_ju_j(\boldsymbol{r})=\mathcal{L}u_j(\boldsymbol{r})+\int d\boldsymbol{r}'V(\boldsymbol{r}'-\boldsymbol{r})n(\boldsymbol{r}',\boldsymbol{r})u_j(\boldsymbol{r}')+N_0\int d\boldsymbol{r}'\phi(\boldsymbol{r}')V(\boldsymbol{r}'-\boldsymbol{r})v(\boldsymbol{r}')\phi(\boldsymbol{r}),\tag{6a}$$

$$E_jv_j(\boldsymbol{r})=\mathcal{L}v_j(\boldsymbol{r})+\int d\boldsymbol{r}'V(\boldsymbol{r}'-\boldsymbol{r})n(\boldsymbol{r},\boldsymbol{r}')v_j(\boldsymbol{r}')+N_0\int d\boldsymbol{r}'\phi(\boldsymbol{r}')^*V(\boldsymbol{r}'-\boldsymbol{r})u(\boldsymbol{r}')\phi(\boldsymbol{r})^*.\tag{6b}$$

The quasiparticle annihilation and creation operators α_j and $\alpha_j^\dagger$ satisfy the usual Bose commutation relations.

In terms of u's and v's, the thermal density correlation function is written as

$$\tilde{n}(\boldsymbol{r}',\boldsymbol{r})=\sum_j[u_j^*(\boldsymbol{r}')u_j(\boldsymbol{r})+v_j(\boldsymbol{r}')v_j^*(\boldsymbol{r})]N_{ex}(E_j)+v_j(\boldsymbol{r}')v_j^*(\boldsymbol{r}),\tag{7}$$

where $N_{ex}(E_j)$ is the Bose distribution for the quasiparticle excitations:

$$N_{ex}(E_j)\equiv\langle\hat{\alpha}_j^\dagger\hat{\alpha}_j\rangle=\frac{1}{\exp\left(\frac{E_j}{k_BT}\right)-1}.\tag{8}$$

The expression for $\tilde{n}(\boldsymbol{r})$ in terms of u and v is obtained by setting $\boldsymbol{r}'=\boldsymbol{r}$ in Eq. (7). Similar expressions may be easily obtained for the total and release energy of the condensate in the trap.

As usual, the self-consistent HFB-Popov equations (3) and (6) are solved iteratively. At first, one sets $\tilde{n}(\boldsymbol{r}',\boldsymbol{r})=\tilde{n}(\boldsymbol{r})=0$. The thermal component contribution is then updated at each further step using Eq. (7) until convergence is reached.

It can be appreciated that long-range interactions present a significant challenge to the computational implementation of the HFB-Popov method. The difficulties arise even for zero temperature, where (ignoring the negligible quantum depletion) the HFB-Popov equations reduce to the Bogoliubov–de Gennes (BdG) equations, which due to the long-range exchange interactions, are now integro-differential rather than simply differential equations. In Ref. [13] we have introduced a new algorithm, which enabled us to solve the BdG equations for a gas with dipolar interactions in a 3D trap with cylindrical symmetry, by utilizing the cylindrical symmetry to reduce the effective dimensionality of the problem from 3D to 2D. For the finite temperatures with which the HFB-Popov method is concerned, the long-range interactions introduce an additional difficulty: Equations (3) and (6) involve not only the thermal density $\tilde{n}(\boldsymbol{r})$, but also the thermal correlation function $\tilde{n}(\boldsymbol{r}',\boldsymbol{r})$. The most difficult terms are

those involving the long-range exchange interaction such as $\int d\boldsymbol{r}' V(\boldsymbol{r}'-\boldsymbol{r}) n(\boldsymbol{r}',\boldsymbol{r}) u_j(\boldsymbol{r}')$ in Eq. (6b). In the case where there is no thermal component, the total correlation function is expressed as a direct product: $n(\boldsymbol{r}',\boldsymbol{r})=\phi^*(\boldsymbol{r}')\phi(\boldsymbol{r})$. In this case, the above exchange term may be effectively evaluated by the use of Hankel-Fourier transform [13]. In the presence of a thermal component, the total correlation function does not have such a direct product decomposition. It might be possible to circumvent this complication by direct evaluation of the exchange integral on a spatial grid (without resort to Fourier transforms; see, for example, [23])—however, this is complicated by the singular nature ($1/\boldsymbol{r}^3$behavior) of dipolar interactions at the origin.

To obtain a feasible numerically solvable problem, we therefore make an additional approximation: in Eqs. (3) and (6) we let $\tilde{n}(\boldsymbol{r}',\boldsymbol{r})=0$ for $\boldsymbol{r}'\neq\boldsymbol{r}$, or equivalently, we let $n(\boldsymbol{r}',\boldsymbol{r})=\phi(\boldsymbol{r}')^*\phi(\boldsymbol{r})$. Physically, in Eq. (3) this amounts to ignoring the forces on the condensed part due to the long-range exchange interaction with the thermalized part. In Eq. (6) this amounts to ignoring the long-range exchange interaction between the thermal component of the gas and itself. On the other hand, in Eq. (6) we do take into account the effect on excitation modes and frequencies due to the long-range exchange interaction with the condensate. We treat exactly the long-range direct interactions which involve $n(\boldsymbol{r})$. We also treat exactly the short-range (contact) interaction, for which the exchange and direct terms are identical.

A partial justification for the above scheme may be found in the good agreement between the "two-gas model" of dilute BECs and the full HFB-Popov description for gases with short-range interactions [24]. In the two-gas description, the condensate wave function is that of a $T=0$ BEC with the appropriate (depleted) number of condensate atoms N_0 and the surrounding thermal cloud is described by the statistical mechanics of an ideal gas in the combined potentials of the trap and the cloud-condensate interaction. The full HFB-Popov description may be reduced to the two-gas description by letting $\tilde{n}(\boldsymbol{r},\boldsymbol{r}')=0$ for all $\boldsymbol{r},\boldsymbol{r}'$, so that, in particular, $\tilde{n}(\boldsymbol{r})\equiv\tilde{n}(\boldsymbol{r},\boldsymbol{r})=0$. The reason for the success of the two-gas model seems to derive from the fact that the thermal component is typically much more dilute than the condensate part. Therefore, to a good approximation, it may be described as an ideal gas. The approach suggested above for the treatment of dipolar BEC at $T>0$ may be described as treating the thermal component as "partly ideal"—i.e., "ideal" only with respect to long-range exchange interactions. Thus, it is a compromise between the full HFB-Popov method and the two-gas description.

Moreover, we note as a general thermodynamical property that the correlation function $\tilde{n}(\boldsymbol{r}',\boldsymbol{r})$ naturally decreases towards zero with increase in temperature (for $\boldsymbol{r}'\neq\boldsymbol{r}$). Thus, with increasing temperature, it makes sense to ignore the thermal long-range exchange interaction which is due to the correlation function of the thermal component of the gas.

The number of excitation modes that need to be taken into account in Eq. (6b) in order to saturate the thermal cloud density is very large (tens of thousands). For the higher excitation modes, the semiclassical description has proved very useful and accurate [13,25]. Thus, we follow the approach of solving Eqs. (6) for discrete modes up to an appropriate energy cutoff and using their semiclassical version [13] for modes above this energy cutoff. The energy cutoff is typically somewhat larger than the chemical potential and is adjusted in each specific case until convergence is achieved.

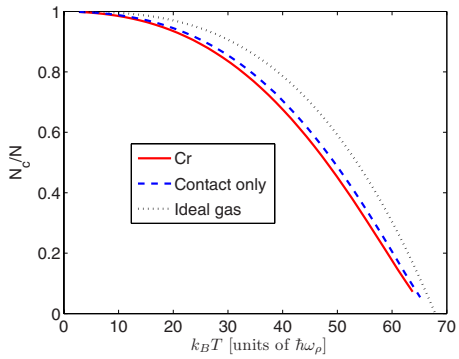

FIG. 1. (Color online) Condensate fraction as a function of temperature in a pancake trap with aspect ratio 1:4 (i.e., $\omega_\rho/\omega_z=1/4$): unpolarized, i.e., dipole moment set to zero (dashed line), polarized (solid line), and ideal gas (dotted line). The total number of ^{52}Cr atoms is 100 000.

III. RESULTS

A. Cr in a pancake trap

We first study the effects of temperature for a ^{52}Cr gas in a trap with frequencies $\omega_\rho=2\pi\times 100$ Hz and $\omega_z=2\pi\times 400$ Hz (a pancake trap). The magnetic-dipole moment of polarized Cr is relatively large for atoms, 6-bohr magnetons. However, the resulting dipole-dipole interaction is still small compared to the strength of the short-range interaction (scattering length $a=96a_0$ [26]). A useful parameter here is the dimensionless quantity $\epsilon_{dd}=\frac{md^2}{3\hbar^2/a}$. A homogeneous condensate is unstable if $\epsilon_{dd}>1$ [27]. For Cr, $\epsilon_{dd}=0.16$. However, using a Feshbach resonance, it is possible to reduce the scattering length and thus increase the dipolar effects [31]. For the present study we assume a reduced scattering length of $20a_0$, so that $\epsilon_{dd}=0.8$. The number of atoms in the trap is taken to be 10^5.

In Fig. 1 we show the condensate fraction in the pancake trap as a function of temperature. For comparison, we have included results of an unpolarized gas by setting the dipole moment $d=0$. It is seen that the effect of the polarization of the gas is to decrease the condensate fraction at any given temperature, compared to the nonpolarized gas. As a result the critical temperature is also reduced. This effect may be expected since in a pancake trap the average dipolar interaction is repulsive; thus, the thermal effect due to polarization is similar to that of increasing the scattering length.

In Fig. 2 we plot the eigenfrequencies of the lowest collective modes. Although the dipolar interaction causes large shifts in the frequencies, the temperature dependence of these shifts is very small, except very near the critical temperature. The shift in frequencies due to polarization is, qualitatively, similar to that of increasing the effective short-

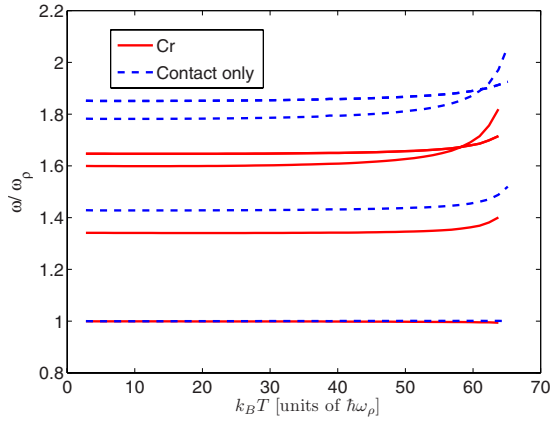

FIG. 2. (Color online) Lowest excitation frequencies a function of temperature for a ^{52}Cr condensate in a pancake trap with aspect ratio 1:4: polarized (solid lines) and unpolarized (dashed lines). For each angular momentum number $m=0,1,2,3$, we plot only the lowest mode with this m.

range repulsion. Note the Kohn mode $(\omega/\omega_\rho=1)$ which should remain constant at 1. The slight deviation from 1 at higher temperatures is due to Popov approximation which in effect computes the dynamics of the condensate in the presence of a static thermal component. A more correct description should treat both components dynamically. Nevertheless, the deviation of the Kohn mode from the theoretical value of 1 is small.

B. Cr in a cigar trap

Figures 3 and 4 show the condensate fraction and lowest collective-mode frequencies as a function of temperature for a ^{52}Cr gas in a cigar trap with $\omega_z=2\pi\times 100$ Hz and $\omega_\rho=2\pi\times 400$ Hz (with a reduced scattering length $a=20a_0$ as before). Notice that now the effect of the dipolar interaction is to increase the condensate fraction at any given temperature, thus increasing also the critical temperature for the onset of condensation. Again, this can be understood due to the dipolar interaction being effectively attractive in a cigar geometry. Similar to the case of a pancake trap, the dipolar interaction leads to significant shift in the frequencies of the low modes, but these shifts depend only weakly on temperature.

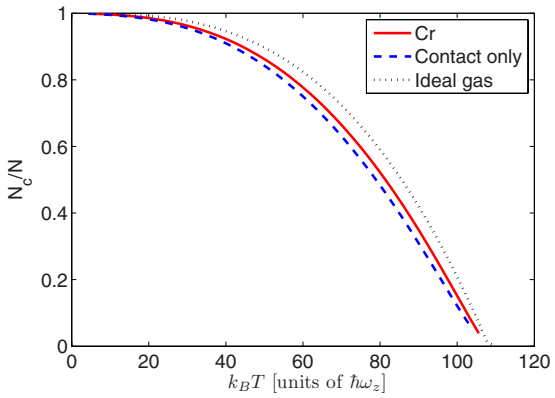

FIG. 3. (Color online) Condensate fraction as a function of temperature in a cigar trap with aspect ratio 4:1: unpolarized (dashed line), polarized (solid line), and ideal gas (dotted line).

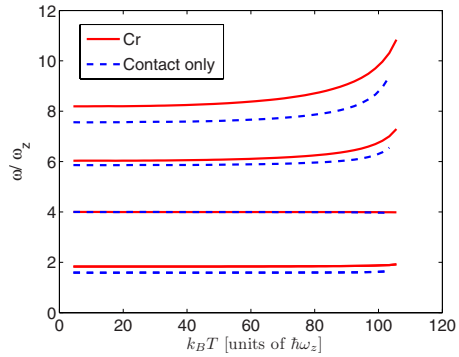

FIG. 4. (Color online) Lowest excitation frequencies as a function of temperature for a ^{52}Cr condensate in a cigar trap with aspect ratio 4:1: polarized (solid lines) and unpolarized (dashed lines). Only modes which are even in the z direction are shown. For each angular momentum number $m=0,1,2,3$, we plot only the lowest even mode with this m.

C. Biconcave condensates

We now turn to examine the finite-temperate effects on the biconcave-shaped condensate reported in Ref. [2]. There, we found an interesting novel structure of pure dipolar condensates in pancake traps at zero temperature. For an appropriate choice of parameters, the condensate density does not obtain its maximum in the center of the trap. Rather, the maximum density is obtained along a ring and the center of the trap is the local minimum of the density. This gives rise to a biconcave condensate shape similar to that of a red-blood cell. Recently, other shapes have been predicted in noncylindrically symmetric traps [28]. In this section, we investigate the temperature effect on the biconcave condensate in a cylindrically symmetric trap.

In Fig. 5 we plot the condensate fraction as a function of temperature for a pure ^{52}Cr dipolar condensate (i.e., where the scattering length has been tuned to zero via a Feshbach resonance) in a pancake trap with aspect ratio $\omega_\rho/\omega_z=1/7$. For number of particles $N=16\,300$, a biconcave structure is formed at $T=0$. In this figure it is notable that the dipolar interaction brings about significant change (about 10%) in the condensate fraction for temperatures of order half the critical temperature. Yet the critical temperature itself is almost unchanged. Indeed, the analytical formula of Refs. [29,30] predicts a very small reduction of 0.5% in the critical temperature.

An interesting question is, what happens to the biconcave structure with the increase in temperature? The biconcave shape eventually washes out by $T=T_c$, yet (as we shall show) the shape persists to surprisingly high temperature. To study this, we define a contrast parameter $c=1-n(0)/n_{\max}$, where $n(0)$ is the central density and n_{max} is the maximal density. For a normal density profile where the maximal density is

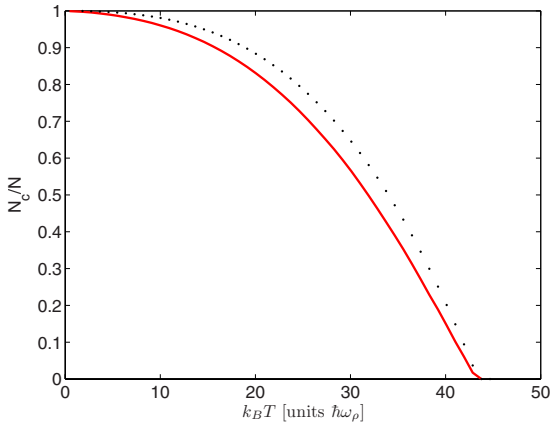

FIG. 5. (Color online) Condensate fraction as a function of temperature in a pancake trap with aspect ratio 1:7, for which biconcave structure is formed at $T=0$: polarized (solid line) and ideal gas (dotted line). The total number of ^{52}Cr atoms is 16 300. The scattering length is assumed tuned to 0.

obtained at the center, $c=0$. In Fig. 6 we plot the biconcave structure parameter for the total density profile, as well as for the condensed part alone, as a function of temperature. It is seen that when the temperature approaches about 70% of the critical temperature, the biconcave structure disappears. Generally, one would expect the disappearance of the biconcave structure due to the thermal excitations. We note that according to Ref. [2], the biconcave contrast (at $T=0$) is reduced with decreased number of particles. Thus, when the condensate is depleted, we also expect the biconcave parameter to decrease. For $T>0.15T_c$, this is indeed the case. But for lower temperatures, we see that the biconcave contrast, for both the total density and the condensed part alone, slightly increases with temperature.

To understand this effect, let us first consider the density profile of the thermal cloud alone. Consider first the simplest

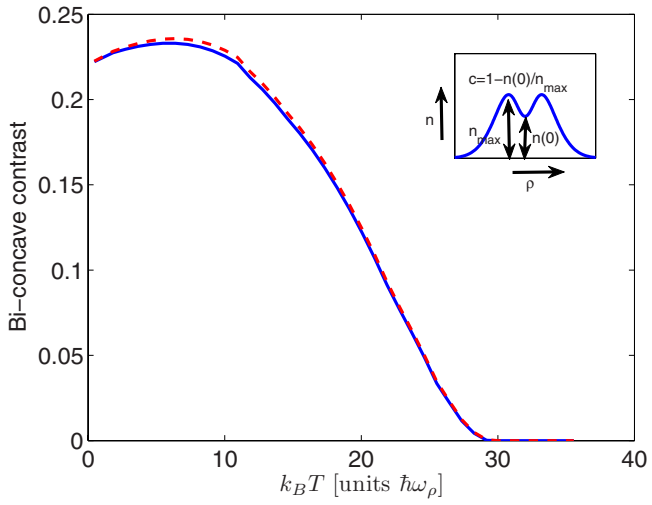

FIG. 6. (Color online) Biconcave contrast as a function of temperature in a pancake trap with aspect ratio 1:7. Solid line: contrast parameter for the total density. Dashed line: contrast parameter for the condensed part. Inset: illustration of a typical biconcave density profile showing how the biconcave contrast c is defined.

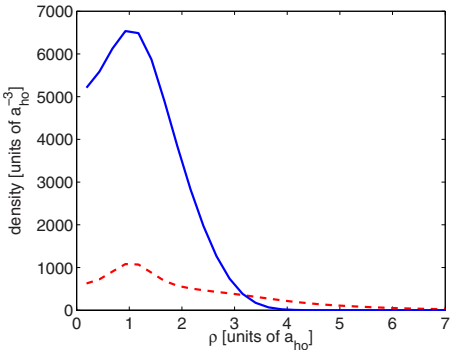

FIG. 7. (Color online) Radial density profiles of the condensate density (solid line) and 10× the thermal component density (dashed line). Note that we scaled the thermal component density by a factor of 10 for visual comparison. The trap aspect ratio is 1:7 as in Fig. 6, and the temperature is $T=0.2T_c$, where T_c is the critical temperature.

case of an ideal gas in a harmonic trap. The thermal cloud occupies harmonic oscillator states according to Bose statistics. The lowest and most populated excited state, one above the ground state, has a node at the center of the trap. Thus, at low temperatures, one expects the thermal cloud to have reduced density at the center of the trap, even in the absence of repulsive short-range interactions. This effect is easily verified by numerical simulations and is seen to be more pronounced when the dimensionality is reduced, such as in highly pancake or cigar traps. Of course, for an ideal gas, the total density (thermal+condensate) still has its maximum at the center.

Consider now the dipolar gas. As the temperature is raised from $T=0$, the lowest and most populated thermal gas mode is a sloshing (Kohn mode) with a node in the center. Thus for low temperatures the thermal component has lower density at the center, as is demonstrated in Fig. 7. The thermal component creates in turn a mean field, which is shown in Fig. 8. It shows that the maximum mean-field potential is obtained

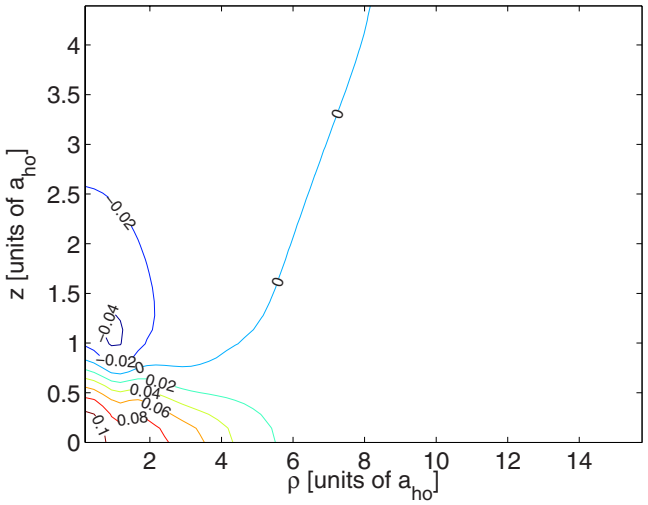

FIG. 8. (Color online) The mean dipolar field due to the thermal component density whose radial profile is shown in Fig. 7.

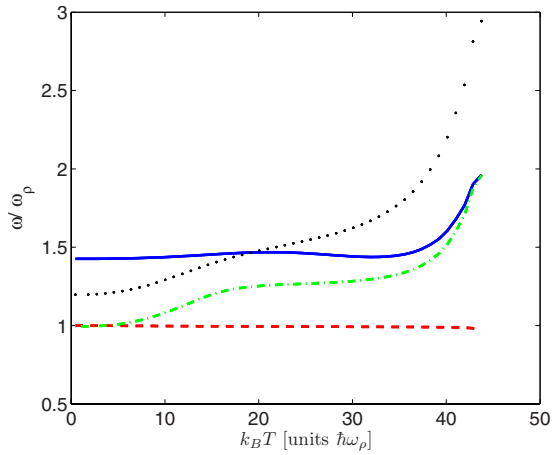

FIG. 9. (Color online) Lowest excitation frequencies as a function of temperature for a ^{52}Cr condensate in a pancake trap with aspect ratio 1:7. Solid line: lowest $m=0$ mode. Dashed line: $m=1$ mode. Dash-dotted line: $m=2$ mode. Dotted line: $m=3$ mode.

in the center of the trap, even though this is not where the place of maximum thermal component density. This is due to the long-range nature of the dipolar interaction: the contributions from the ring of maximal density of the thermal cloud add together in the center of trap. The mean field due to the thermal cloud causes the condensate part to be repelled from the center. The result is that the biconcave contrast of the condensate is larger than it would have been with the same number of condensed particles in a pure harmonic trap with no thermal component. This gives rise to the behavior seen in Fig. 6 at low temperatures.

A caveat is that, as mentioned above, we made an approximation in our computations by ignoring thermal exchange effects. This may, in principle modify the effect of the thermal component on the condensed part, at low temperatures in particular. Exploring the effect of the thermal exchange interaction would require a considerably heavier computation than undertaken in this current work.

In Fig. 9 we plot the lowest excitation frequencies as a function of temperature for the pancake trap with aspect ratio 1:7 (containing the above-mentioned biconcave structure). The $m=1$ is as usual the Kohn mode. Note that at $T=0$ the $m=2$ and $m=3$ modes are lower than the $m=1$ mode. The near degeneracy of the $m=1$ and $m=2$ modes at $T=0$ is accidental: for a higher number of particles, the $m=2$ and $m=3$ modes actually go below the $m=1$ mode, a consequence of the discrete rotonlike spectrum discussed in Ref. [2]. Close to the critical temperature the excitation energies approach their ideal gas values, as might be expected due to the decreasing density of the gas. In between there is an interesting crossing between the $m=0$ and $m=3$ modes.

D. Comparison with Monte Carlo simulations

Finally, we have attempted to compare the HFB-Popov method with the path-integral Monte Carlo simulations of Nho and Landau [9]. However, we do not find a good agreement. The energies with HFB-Popov approximation for a dipolar condensate in a pancake trap came about 10% higher than the Monte Carlo simulation, with a similar discrepancy in the shape (width) of the dipolar condensates. We note that the Monte Carlo simulations were performed for a very small number of particles, between 27 and 125. Under these conditions, the critical temperature is very small, of the order of the trap frequencies, and in fact lower than the chemical potential. Thus, only a few low modes are excited even close to the critical temperature T_c. At the simulated temperature of $0.4T_c$ the density of the thermal gas is of the order of that of the condensate and there is a large overlap between the two. Under these conditions it may be expected that the approximation of ignoring the thermal-thermal dipolar exchange interactions is invalid. Thus, it is plausible that the disagreement is due to this additional approximation rather than the inadequacy of the HFB-Popov method. But for a number of particles of the order of 10^4–10^5, the critical temperature is much higher than the trap frequencies and the density of the thermal cloud significantly lower than that of the condensate. Thus, we believe our method should still give valid results under normal experimental conditions.

IV. CONCLUSIONS

In conclusion, we applied the Hartree-Fock-Bogoliubov-Popov approximation to dipolar gases in harmonic, cylindrically symmetric traps. For computational reasons, the exchange interaction due to the thermal gas has to be ignored (i.e., we ignore exchange interaction due to long-range spatial correlation in the thermal component). For normal configurations where the condensate structure at $T=0$ has a maximum at the center, we observe a temperature-dependent behavior similar to that of a gases with contact interaction [19,20], but the behavior depends on the aspect ratio of the trap: for pancake traps, the dipolar interaction is effectively repulsive, leading to reduction of condensed part at a given temperature and thus also a reduction of the critical temperature for condensation, while in a cigar trap, it is effectively attractive, leading to the opposite thermal effects. For configurations where biconcave structure exists at $T=0$, we find the somewhat surprising result that this structure is actually enhanced at low temperatures (i.e., the ratio of the central density to the maximal density is reduced). For higher temperatures, the biconcave structure gradually becomes less distinct and it disappears at a temperature of about 75% of the critical temperature. The low excitation spectrum of the biconcave structure also shows interesting temperature dependence with crossing between different modes.

ACKNOWLEDGMENT

We gratefully acknowledge financial support from the NSF.

[1] J. Stuhler, A. Griesmaier, T. Koch, M. Fattori, T. Pfau, S. Giovanazzi, P. Pedri, and L. Santos, Phys. Rev. Lett. **95**, 150406 (2005).
[2] S. Ronen, D. C. E. Bortolotti, and J. L. Bohn, Phys. Rev. Lett. **98**, 030406 (2007).
[3] S. Yi and L. You, Phys. Rev. A **61**, 041604(R) (2000).
[4] K. Góral, K. Rzążewski, and T. Pfau, Phys. Rev. A **61**, 051601(R) (2000).
[5] M. Baranov, L. Dobrek, K. Góral, L. Santos, and M. Lewenstein, Phys. Scr. **T102**, 74 (2002).
[6] K. Góral and L. Santos, Phys. Rev. A **66**, 023613 (2002).
[7] L. Santos, G. V. Shlyapnikov, and M. Lewenstein, Phys. Rev. Lett. **90**, 250403 (2003).
[8] D. H. J. O'Dell, S. Giovanazzi, and C. Eberlein, Phys. Rev. Lett. **92**, 250401 (2004).
[9] K. Nho and D. P. Landau, Phys. Rev. A **72**, 023615 (2005).
[10] N. R. Cooper, E. H. Rezayi, and S. H. Simon, Phys. Rev. Lett. **95**, 200402 (2005).
[11] J. Zhang and H. Zhai, Phys. Rev. Lett. **95**, 200403 (2005).
[12] S. Yi and H. Pu, Phys. Rev. A **73**, 061602(R) (2006).
[13] S. Ronen, D. C. E. Bortolotti, and J. L. Bohn, Phys. Rev. A **74**, 013623 (2006).
[14] M. Takahashi, S. Ghosh, T. Mizushima, and K. Machida, Phys. Rev. Lett. **98**, 260403 (2007).
[15] Y. Kawaguchi, H. Saito, and M. Ueda, Phys. Rev. Lett. **96**, 080405 (2006).
[16] S. Yi and H. Pu, Phys. Rev. Lett. **97**, 020401 (2006).
[17] I. E. Mazets, D. H. J. O'Dell, G. Kurizki, N. Davidson, and W. P. Schleich, J. Phys. B **37**, S155 (2004).
[18] A. Griffin, Phys. Rev. B **53**, 9341 (1996).
[19] D. A. W. Hutchinson, E. Zaremba, and A. Griffin, Phys. Rev. Lett. **78**, 1842 (1997).
[20] R. J. Dodd, M. Edwards, C. W. Clark, and K. Burnett, Phys. Rev. A **57**, R32 (1998).
[21] A. J. Leggett, Rev. Mod. Phys. **73**, 307 (2001).
[22] B. D. Esry, Phys. Rev. A **55**, 1147 (1997).
[23] S. Yi and L. You, Phys. Rev. A **63**, 053607 (2001).
[24] R. J. Dodd, M. Edwards, and C. W. Clark, J. Phys. B **32**, 4107 (1999).
[25] J. Reidl, A. Csordás, R. Graham, and P. Szépfalusy, Phys. Rev. A **59**, 3816 (1999).
[26] A. Griesmaier, J. Stuhler, T. Koch, M. Fattori, T. Pfau, and S. Giovanazzi, Phys. Rev. Lett. **97**, 250402 (2006).
[27] C. Eberlein, S. Giovanazzi, and D. H. J. O'Dell, Phys. Rev. A **71**, 033618 (2005).
[28] O. Dutta and P. Myestre, e-print arXiv:cond-mat/0703044.
[29] K. Glaum, A. Pelster, H. Kleinert, and T. Pfau, Phys. Rev. Lett. **98**, 080407 (2007).
[30] K. Glaum and A. Pelster, Phys. Rev. A **76**, 023604 (2007).
[31] T. Pfau (private communication).